sustainability

MDPI

Article

Sustainable Utilization of Waste Pumice Powder in Slag-Based Geopolymer Concretes: Fresh and Mechanical Properties

Zrar Safari [1,*], Khaleel H. Younis [2,3] and Ibtisam Kamal [4,5]

[1] Department of Civil and Environmental Engineering, Faculty of Engineering, Soran University, Soran 44008, Kurdistan Region, Iraq
[2] Road Construction Department, Erbil Technology College, Erbil Polytechnic University, Erbil 44001, Kurdistan Region, Iraq; khaleel.younis@epu.edu.iq
[3] Civil Engineering Department, Tishk International University, Erbil 44001, Kurdistan Region, Iraq
[4] Department of Chemical Engineering, Faculty of Engineering, Soran University, Soran 44008, Kurdistan Region, Iraq; ibtisam.kamal@soran.edu.iq
[5] Department of Petroleum Engineering, Basrah University College of Science and Technology, Basrah 61004, Iraq
* Correspondence: zrar.mahmood@cive.soran.edu.iq

Abstract: In societies worldwide, there is significant pressure on the construction industry to employ waste/recycled materials instead of natural-sourced materials to develop infrastructures to mitigate negative environmental consequences. This study investigated the feasibility of using waste pumice powder as a binder in place of granular blast-furnace slag to manufacture geopolymer concrete. Three sets of GC mixes were developed with three ratios of alkaline activator/binder (A/B) of 0.45, 0.5, and 0.55. Eight GC mixes were prepared for each set, with eight replacement ratios of GGBFS with WPP (0%, 30%, 50%, 60%, 70%, 80%, 90%, and 100%). The influence of WPP addition as a substitute source of aluminosilicate precursors on the fresh (workability and setting time), mechanical (compressive strength and flexural strength), physical characteristics (density and water absorption), and microstructure morphology of WPP/slag-based geopolymers were studied. A linear correlation between UPV and compressive strength was found. The results revealed that setting times and workability are affected by the A/B ratio and content of WPP. WPP reduces the workability and increases setting time (both initial and final). There was a drop in compressive and flexural strengths as the percentage of WPP in the GC increased. The maximum compressive (60 MPa) and flexural strength (4.96 MPa) at an A/B ratio of 0.45 for a 100% slag content mix were obtained. However, a GC mix containing 50% WPP and 50% slag with a compressive strength of 28 MPa after 28 days of curing at ambient temperature was achieved, which is acceptable for structural applications.

Keywords: alkali activator; geopolymer; GGBFS; waste pumice powder

check for updates

Citation: Safari, Z.; Younis, K.H.; Kamal, I. Sustainable Utilization of Waste Pumice Powder in Slag-Based Geopolymer Concretes: Fresh and Mechanical Properties. *Sustainability* **2024**, *16*, 9296. https://doi.org/10.3390/su16219296

Academic Editor: Antonis A. Zorpas

Received: 26 August 2024
Revised: 13 October 2024
Accepted: 18 October 2024
Published: 25 October 2024

Copyright: © 2024 by the authors. Licensee MDPI, Basel, Switzerland. This article is an open access article distributed under the terms and conditions of the Creative Commons Attribution (CC BY) license (https://creativecommons.org/licenses/by/4.0/).

1. Introduction

As a result of increased cement consumption driven by urban and construction development, the concrete technology sector in the construction industry has been deemed responsible for serious environmental issues such as waste development and carbon dioxide emissions [1–4]. Portland Cement manufacturing produces an average of 600 to 800 kg of CO_2 per ton of cement, which substantially contributes to environmental pollution and further exacerbates the impacts of climate change [5–8]. As stated by the Environmental Protection Agency (EPA), a substantial amount of carbon emissions are released by the cement industry, generating around 7% of worldwide emissions, and it has high energy costs [9,10]. Developing and manufacturing geopolymers, or activated alkali cement, is one strategy for overcoming these issues and substantially decreasing carbon dioxide emissions [11,12]. Since geopolymer concrete (GC) can be produced without the use of ordinary Portland Cement (OPC), it has been characterized as the next generation of concrete because

it contributes less CO_2 emissions [13]. Furthermore, it has been discovered that geopolymer concrete reduces carbon dioxide emissions up to 80%, comparable to OPC concrete [14].

Besides being friendly to the environment, geopolymers, which are solid precursors containing silica and alumina, have been observed to possess good mechanical properties [15–18] and durability performance [19–21], including being resistant to elevated temperatures [22], sulfates and acids [23–25], and an alkali–silica reaction [26], compared to OPC concrete. When all of these benefits are taken into account, GC seems a promising alternative to OPC.

The most well-known alumino-siliceous precursors employed in the synthesis of geopolymers with recognized compositions and behaviors are fly ash [27,28], slag [29,30], metakaolin [31], and calcined clays [32]. Due to their extensive and successful use as pozzolanic materials in the development of mixed OPC and conventional concrete for many years, materials once referred to as by-products, fly ash and GGBFS, are two examples of materials that are no longer considered to be waste [33]. Remarkable progress has been shown in the alkali-activation precursor selection, with a particular emphasis now being devoted to materials that are not highly required, particularly in blends with OPC [34]. A 35–70% reduction in OPC may be achieved in the production of concrete by using GGBS, which has exceptional capabilities to function as cementitious materials when they are finely powdered [35,36]. As a result, geopolymer concrete may be created by blending it with other alkali-activated components [37]. Reduced void formation may be achieved in geopolymer concrete by utilizing GGBS as a precursor [38]. Also, natural pumice has been used alone and in combination with GGBS, metakaolin, and/or slag as precursors in GC in order to improve its properties [39–42]. The setting times (both initial and final) of slag-based GC mixtures dropped when natural pumice was added [43].

To manufacture geopolymers, fly ash, metakaolin, and slag are used. In addition to those precursors, numerous studies examined the possibility of using more geopolymeric materials, such as rice husk ash, volcanic ash, red mud, and waste glass [44].

Nevertheless, the use of construction wastes (CW) as precursors or binders in developing GC mixtures has not been well explored. This is because of their low reactivity, which is mostly caused by the large, irregularly shaped particles that are different from this particular type of precursor [45–50]. According to Komnitsas et al. [51], a powder made from waste tiles was utilized as an influential precursor for geopolymerization, attaining a 57.8 MPa compressive strength after seven days of curing at 80 °C. Research indicated that the application of CW-based ingredients in the production of geopolymers is a rapidly emerging field that needs further focus [52]. Thus, many researchers have examined the way alkali-activation features affect the properties of GC made from construction waste, but the strength and durability of GC with CW have not received as much attention [53].

The present study deals with using pumice waste from the demolition of lightweight pumice blocks in slag-based geopolymers. This investigation examines the strength and physical properties of GC, with a specific focus on the influence of utilizing such waste on workability. The purpose of manufacturing GC is the reuse of the larger available construction waste in recent landfills, and, in order to lower CO_2 emissions, it is crucial to substitute traditional cement. Additionally, it is crucial to acknowledge that the massive amount of solid waste being produced becomes a challenge for worldwide construction. Therefore, the study suggested a possible solution for these issues. Furthermore, as far as the author is familiar with, no investigation has been conducted to evaluate the potential of producing GC combinations that use waste pumice powder obtained by crushing waste blocks. This study is an attempt to produce uncommon green geopolymer binders, which are more environmentally friendly than OPC binders and can be used for numerous applications, providing a competitive alternative to OPC. The study's main purpose is to examine the mechanical and fresh properties of CW-based GC, with different waste pumice powder (WPP) contents, alkaline to binder ratio (A/B) ratios, and curing regimes.

2. Experimental Program

2.1. Materials

2.1.1. Waste Pumice Powder (WPP)

The WPP utilized in this study was collected from waste that was created during the wall construction of a residential building in Erbil, located in the Kurdistan Region, Iraq. This waste is generated during the construction of partition walls made with lightweight pumice blocks. During the construction of the walls, broken pieces of blocks were collected and then screened for plastic and other waste. After that, they were dried under sunlight. Finally, the pieces were crushed into smaller particles and sieved to produce a recycled lightweight pumice aggregate. A Dodge jaw crusher was used in the specialized plant to crush the recycled pumice aggregate and reduce its size in order to produce the powder. As illustrated by Figure 1, the crushed pumice was fed into a ball mill to create waste pumice powder.



Figure 1. Preparation stages of WPP.

An examination of the chemical components of the WPP is shown in Table 1. The results of the X-ray Fluorescence (XRF) and X-ray diffraction (XRD) analyses of the waste pumice powder are shown in Figure 2.

Table 1. Physical properties and chemical compositions of WPP and GGBFS.

Chemical Composition	WPP (wt. %)	GGBFS (wt. %)
SiO_2	45.84	38.159
Al_2O_3	10.24	11.641
Fe_2O_3	2.51	1.591
MgO	5.84	6.675
CaO	31.94	30.966
Na_2O	0.05	1.78
K_2O	3.07	0.8045
TiO_2	0.036	1.51
P_2O_5	0.11	0.07
MnO	0.007	2.295
SO_3	0.11	1.93
Cl	0.12	0.06
LOI	1.27	2.518
Specific gravity (g/cm^3)	2.3	2.9
Fineness (cm^2/g)	4500	5800

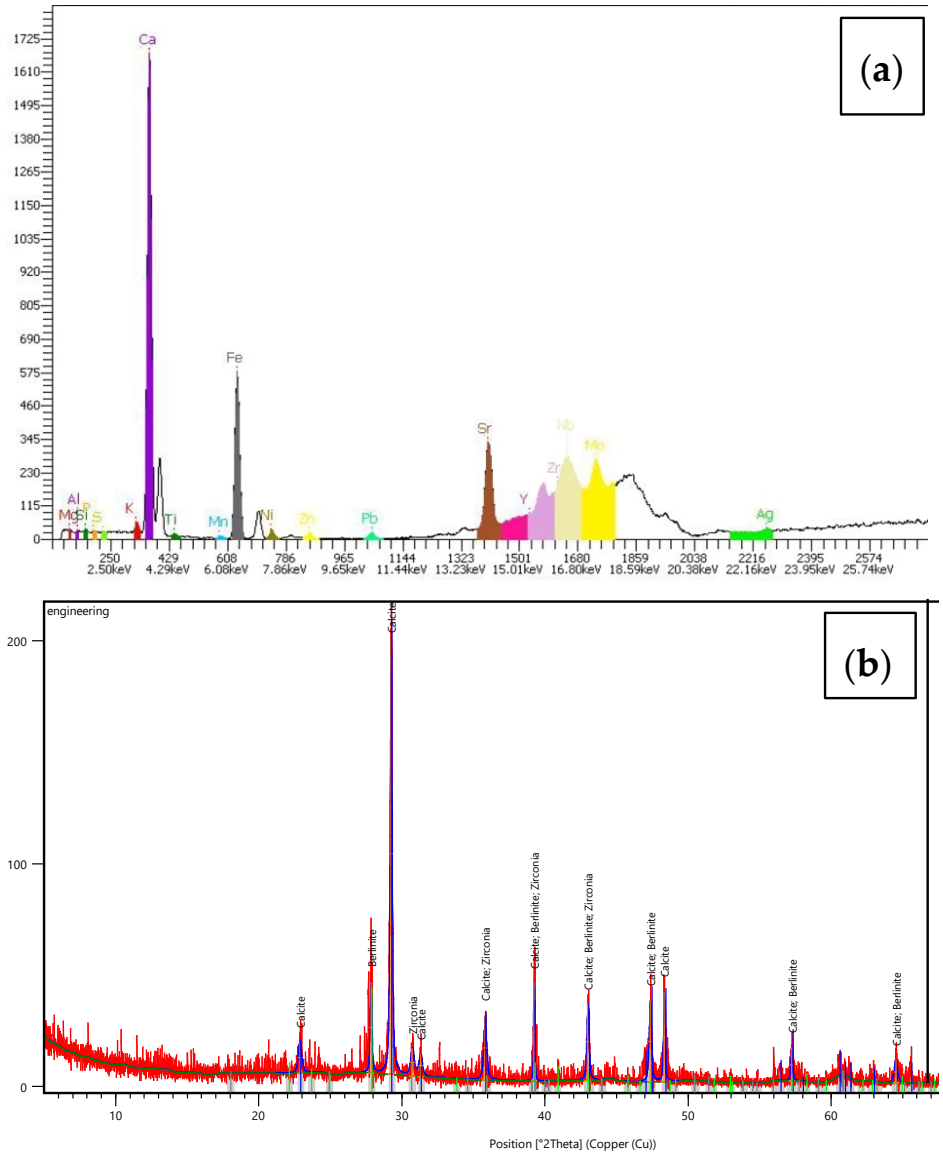

Figure 2. (**a**) XRF, and (**b**) XRD patterns of waste pumice powder.

2.1.2. Ground Granulated Blast-Furnace Slag (GGBFS)

Due to it having higher amounts of calcium oxide (CaO), the current study utilized GGBFS. It enhances the strength and durability characteristics of GC through the curing process at room temperature [54]. The GGBFS was acquired from the Erbil branch of the DCP company. The physical characteristics and chemical composition of GGBFS are displayed in Table 1.

2.1.3. Alkaline Liquid

The alkaline liquid utilized in this experiment was created by mixing sodium hydroxide (NaOH) solution with a solution of sodium-silicate (Na_2SiO_3). The Na_2SiO_3 solution utilized in this investigation has a 1.367 g/cm^3 specific gravity and 3.01 of SiO_2/Na_2O modulus ratio, with chemical components of Na_2O = 9%, SiO_2 = 27.1%, and H_2O, with a mass value of 63.9%. To make the solution, 98% pure NaOH flakes were combined with water. NaOH solutions with a molarity of 12M were made using the laboratory's tap water. For every mixture, a constant $SiO_2/OH-$ ratio of 2 and an alkali activator concentration of 12M were employed. A $SiO_2/OH-$ ratio of 2 was employed in order to produce geopolymer concrete that is both economically viable and has sufficient workability. The alkaline liquid combination was left to rest for a whole day before being utilized to prepare the geopolymer mixes. This was performed by combining the Na_2SiO_3 and NaOH solution utilizing the stirring and mixing apparatus in the laboratory.

2.2. Procedure

A total of twenty-four GC mixes were prepared, each with a different ratio of A/B ratio and a different amount of WPP/GGBFS. A number of trail mixes were made with different amounts of alkali activator and binder. In order to enhance the workability of the fresh GC, the alkali activator, was combined with a high-range water-reducing admixture (MasterGlenium ACE 450 from Sika, Istanbul, Turkey), which included a 2% mass of binder. This was performed before the addition of dry mixes. The geopolymer concrete slurry was mixed for five minutes at room temperature in the laboratory utilizing a 200 L pan mixer. To compact the specimens, a compaction rod was utilized. After casting, the concrete samples were kept at room temperature for 24 h. Table 2 presents the components and quantities of the specimens. The amounts of coarse aggregate, fine aggregate, and water for all of the mixes were 824 kg/m^3, 1047 kg/m^3, and 82 kg/m^3, respectively.

Table 2. Codes and mix proportions of the GCs.

Mix Design of Geopolymer Concrete kg/m^3						
No.	**A/B**	**Precursors**		**FA**	**CA**	**AA**
		WPP	**GGBFS**			
M45–0%	0.45	411.5	0	1047	824.36	185
M45–30%		288.05	123.45			
M45–50%		205.75	205.75			
M45–60%		164.6	246.9			
M45–70%		123.45	288.05			
M45–80%		82.3	329.2			
M45–90%		41.15	370.35			
M45–100%		0	411.5			
M50–0%	0.5	411.5	0	1047	824.36	205.75
M50–30%		288.05	123.45			
M50–50%		205.75	205.75			
M50–60%		164.6	246.9			
M50–70%		123.45	288.05			
M50–80%		82.3	329.2			
M50–90%		41.15	370.35			
M50–100%		0	411.5			
M55–0%	0.55	411.5	0	1047	824.36	226
M55–30%		288.05	123.45			
M55–50%		205.75	205.75			
M55–60%		164.6	246.9			
M55–70%		123.45	288.05			
M55–80%		82.3	329.2			
M55–90%		41.15	370.35			
M55–100%		0	411.5			

M, (mix); A, (alkaline); B (binder); CA, (coarse aggregate); FA, (fine aggregate); AA, (alkaline activator).

For the purpose of preventing the loss of water during the process of curing, the test specimens were vacuum-bagged after casting. The process of curing for all specimens was conducted at ambient temperature and at 60 °C in a dry oven after resting for a whole day at ambient temperature. The concrete specimens were exposed to temperatures up to 60 °C for 24 h; following that, they were stored at ambient temperature until the testing dates of the 7th, 28th, and 180th day.

2.3. Testing

To assess the performance of the produced GC mixtures and investigate the influences of the A/B ratio and the WPP/GGBFS content, a number of experiments on both fresh and hardened concrete were conducted. The ASTM C191-13 standards were implemented in measuring setting times (both the initial and final) to be able to evaluate the fresh characteristics of all geopolymer pastes [55]. After mixing all materials in the fresh stage, the slump cone test was conducted according to ASTM C143 [56]. After performing the slump cone test, the necessary prisms and cubes of the desired size were cast. Three cube specimens (100 × 100 × 100 mm) were subjected to compressive strength with 0.5 kN/s loading rate according to BS EN 12390-3 [57] at curing ages of 7, 28, and 180 days. The flexural strength tests were performed on 400 × 400 × 100 mm prisms in accordance with ASTM D6272 at the age of 28 days [58]. A standard four-point bending test was applied to the specimens in compliance with the specifications given by ASTM.

There were three prisms for each parameter that were tested in order to assess the effect that the A/B ratio and the amount of WPP had on the flexural strength of GC. The samples conducted testing for water absorption after 28 days. To determine the density and water absorption of hardened concrete cubes for each mix after curing according to ASTM C642-21 [59], three specimens of the concrete cubes for each design mix were measured, and the average was recorded. To investigate the strength and homogeneity of the specimens' matrix, an ultrasonic pulse velocity (UPV) test was also performed as part of this study. The UPV test was also carried out to relatively assess the performance of the developed GC mixes for compressive strength. Microstructure analysis was also performed to study the morphology of GC samples. Furthermore, an investigation was conducted into the effects of curing temperature and duration on the strength characteristics of a GC made from pumice powder.

3. Results and Discussion

3.1. Fresh Properties of GC

3.1.1. Setting Times

Compared with conventional concrete, geopolymer concrete has different setting properties. The chemical reaction between the components of aluminosilicate and the alkali activator is responsible for the setting process of geopolymer concrete [60]. The duration of time needed for geopolymer concrete to set depends on a number of variables, which include the binder type used, the amount of alkali activator used, and the curing conditions [61]. Figure 3 shows that setting times (both initial and final) decrease as the ratio of A/B increases from 0.45 to 0.5, regardless of the influences of the type of binder. The finial setting time also decreases when the A/B ratio decreases (Figure 3). The setting time of GC is influenced by both the quantity and composition of the binder used, since it influences the chemical reaction level. This proposes that a decrease in A/B ratios leads to a longer setting process. For example, the initial setting time of the GC (M45–100%) is (153 min) while the initial setting time of M50–100% is (96 min). Setting times decrease with increased alkali activator content; however, a smaller amount will result in increased setting time; similar results were recorded in previous studies [62].

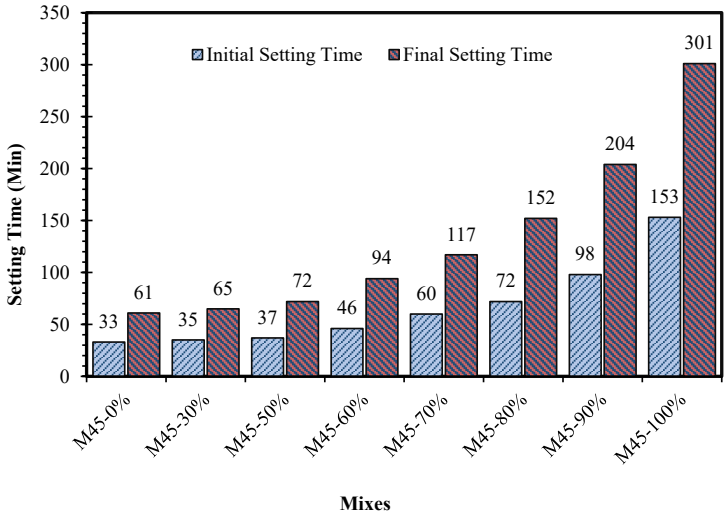

(**a**) 0.45 A/B ratio

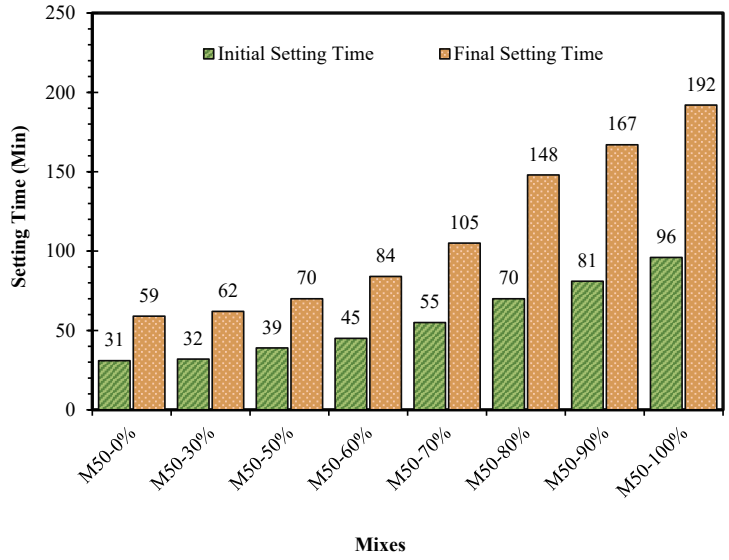

(**b**) 0.50 A/B ratio

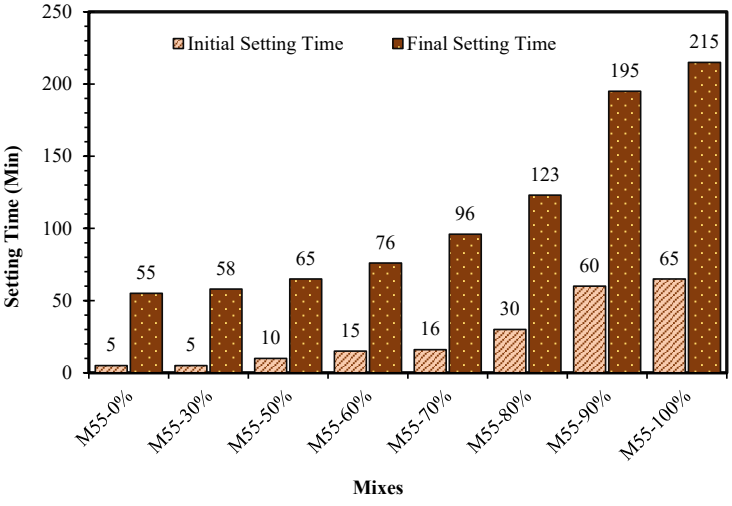

(**c**) 0.45 A/B ratio

Figure 3. The effect of different A/B ratios and the replacement ratios of WPP with GGBFS on the setting time of GC.

Figure 3 shows that the geopolymer setting time is comprehensively influenced by the substantial content of silica and alumina (silica/alumina) ratio of the binder ratio. Geopolymers containing higher replacement levels of WPP (100%) had longer initial setting times (153, 93 and 65 min) along with final setting times (301, 192, 215 min) for alkaline activators of 0.45, 0.5, and 0.55, respectively. The initial setting time increases by 91% when the GGBFS is replaced with WPP by 70% for an A/B ratio of 0.45. Hence, the negative impact of the fast setting of GGBFS-based geopolymer pastes can be mitigated by adding WPP. Figure 3 indicates that regardless of the ratio of A/B, utilizing a higher amount of the WPP results in higher setting times (both initial and final). According to a study, when the mixture has a high SiO_2/Al_2O_3 ratio, the formation of silicate oligomers in the alkali environment means that an extended period of time is needed for condensation to create the geopolymer network, which ultimately interferes with the setting process [63].

3.1.2. Workability

GC is known to have a lower workability (more dense and cohesive than OPC concrete); this presents one of the primary challenges of its use [64]. Therefore, a superplasticizer and more water must be used to enhance workability [65]. Figure 4 displays the slump values for each fresh geopolymer concrete mixture. Generally, the findings show that despite the WPP content, fresh geopolymer concrete is more workable when the A/B ratio is raised from 0.45 to 0.55. For instance, at the content of 50% of WPP, the slump of the GC mixes increased from (85 mm) to (190 mm) when the ratio of A/B increased from 0.45 to 0.55. Similar results were recorded for the mixes made with other contents of WPP. The increase in the A/B ratio is responsible for this behavior, which can be due to the fact that the fluidity of the mixes increase. A similar result was observed by Gugulothu and Rao [66], where slump values, as the authors reported, increased with increasing A/B ratios. Water is not a necessary component of the geopolymerization process; however, it is often added in practice to increase its workability [67]. The water produced as a result of the geopolymer reaction also plays a role in ensuring the desired workability of the GC mixture [68]. Through another study, it was reported that the slump was not affected directly by the A/B ratio; however, their influence on the liquid content affected the mix design's workability [69].

The results showed a decreasing slump trend with a higher proportion of WPP for all A/B ratios, as shown in Figure 4. For example, at an A/B ratio of 0.55, the slump value declined from (275 mm) to (25 mm) when the WPP content increased from 0% to 100%, respectively. WPP is used as a precursor in the manufacturing of geopolymers; however, during the alkaline-activation process, the irregular shape of WPP reduces its fluidity, which affects the workability and flowability of fresh geopolymer concrete. Additionally, GGFBS concrete entrains less air than activated WPP geopolymer concrete [70]. Slump value rises when GGBFS content in a new mix increase. A similar result was observed by other researchers [71]. The M55–0% mix reached an extreme slump value of 275 mm and, for the GC mix of M45–100%, with a 0.45 A/B ratio, while there was no slag present, the slump value was recorded as 0 mm. When 50% of GGBFS was replaced with WPP, the slump decreased from 165 to 85 mm, 260 to 225 mm, and 275 to 190 mm when the A/B ratios were 0.45, 0.5, and 0.55, respectively. On the other hand, this could be explained by the increase in the ball-bearing impact that occurs within the geopolymer concrete and a reduction in the amount of flocculated pozzolanic particles in the mix [38].

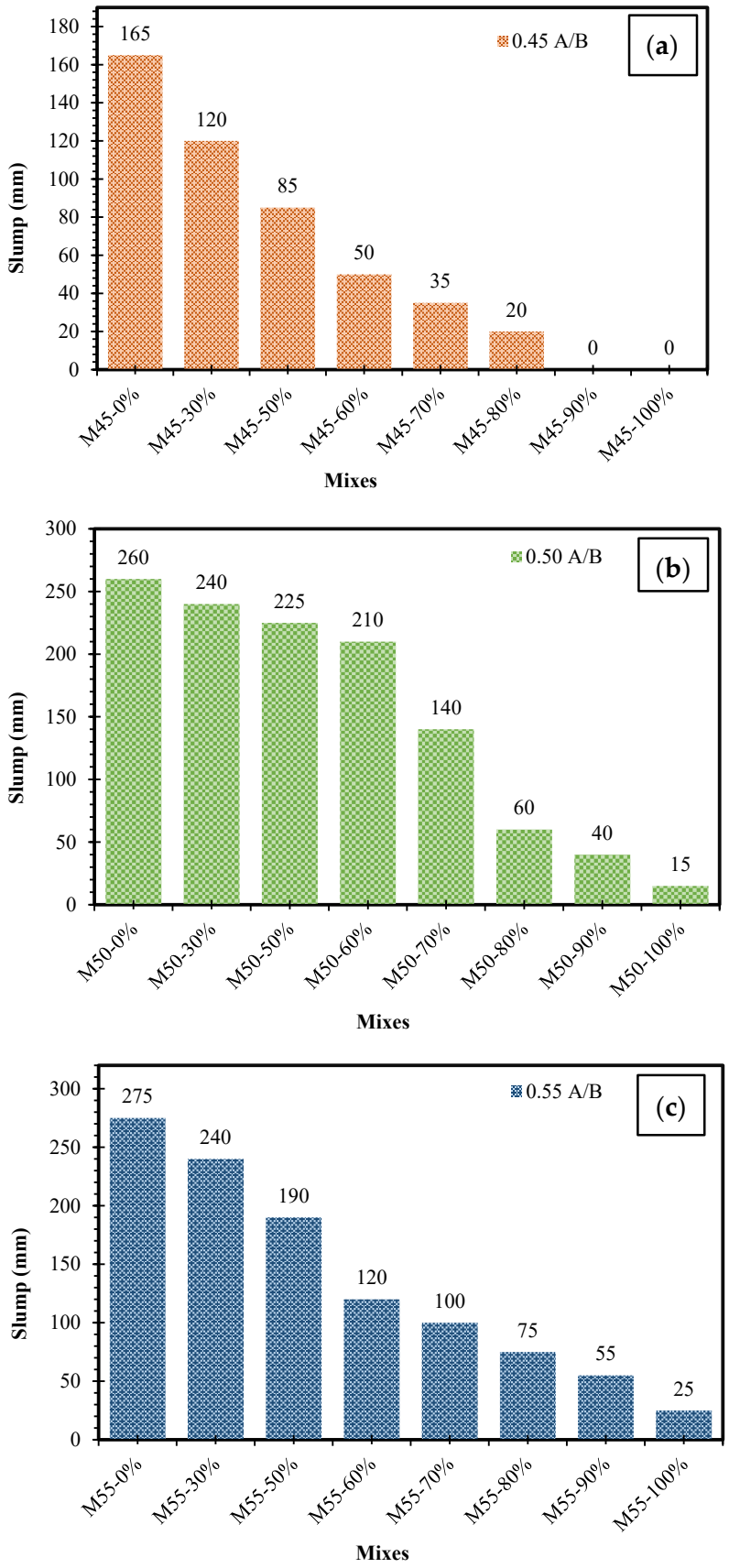

Figure 4. The effect of A/B ratio and WPP content on the slump of GC mixes; (**a**) an A/B ratio of 0.45, (**b**) an A/B ratio of 0.50, and (**c**) an A/B ratio of 0.55.

3.2. Hardened Properties of GC

3.2.1. Density

The average unit weight of each of the GC mix combinations is shown in Figure 5. It demonstrates that, regardless of the binder type, the unit weight of GC mixes decreases as the A/B ratio rises from 0.45 to 0.55. For instance, the density of the slag GC mix decreases by 4% as the A/B ratio rises from 0.45 to 0.55. It was reported that the A/B ratio has a significant influence on the processes of geopolymerization and water dissipation rates of the GPC mix [72]. A GC mix with 60% of WPP shows a similar decreasing trend when increasing the A/B from 0.45 to 0.55, as the density decreases from 2371 kg/m^3 to 2267 kg/m^3, respectively. The findings show that the unit weight of GC mixes decreases as the replacement level of WPP rises. As presented, the slag GC mix has the highest density of 2500.5 kg/m^3 at the age of 28 days in an oven-dry state. The decrease in the density values with increasing WPP content is related to the lower density of the WPP precursor compared to the density of GGBFS.

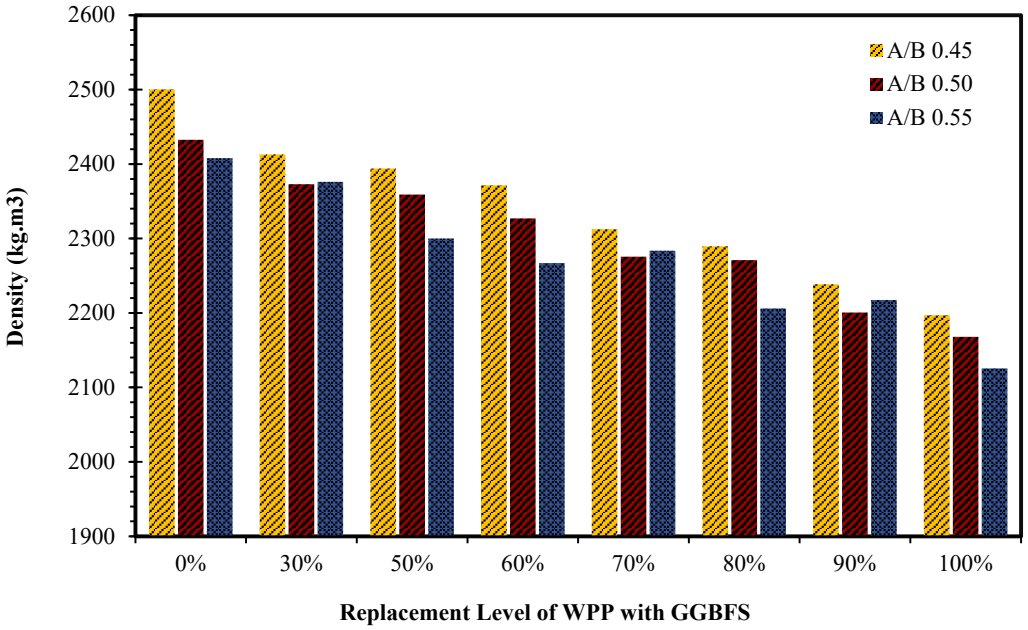

Figure 5. The density of GC mixes with different replacement levels of WPP with GGBS and A/B ratio.

3.2.2. Compressive Strength

The following sections present the compressive strength results of WPP/GGBFS geopolymer concrete with respect to different A/B ratios, WPP content, and curing conditions. The evolution of compressive strength in GC as a function of various mixture design factors is investigated separately.

Effect of A/B Ratio

One of the key parameters to determine the compressive strength of GC is the alkaline activator/binder ratio [73,74]. The A/B ratio statistically substantially influences the compressive strength of the generated GC, as Figure 6 illustrates. Typically, as the ratio of A to B rises, the compressive strength falls. The high water/solid ratio linked to a greater A/B ratio, which can erode the bonds separating solid particles, is the cause of this association. As noticed in Figure 6, increasing the A/B ratio from 0.45 to 0.55 decreased the compressive strength for certain types of precursors and curing conditions.

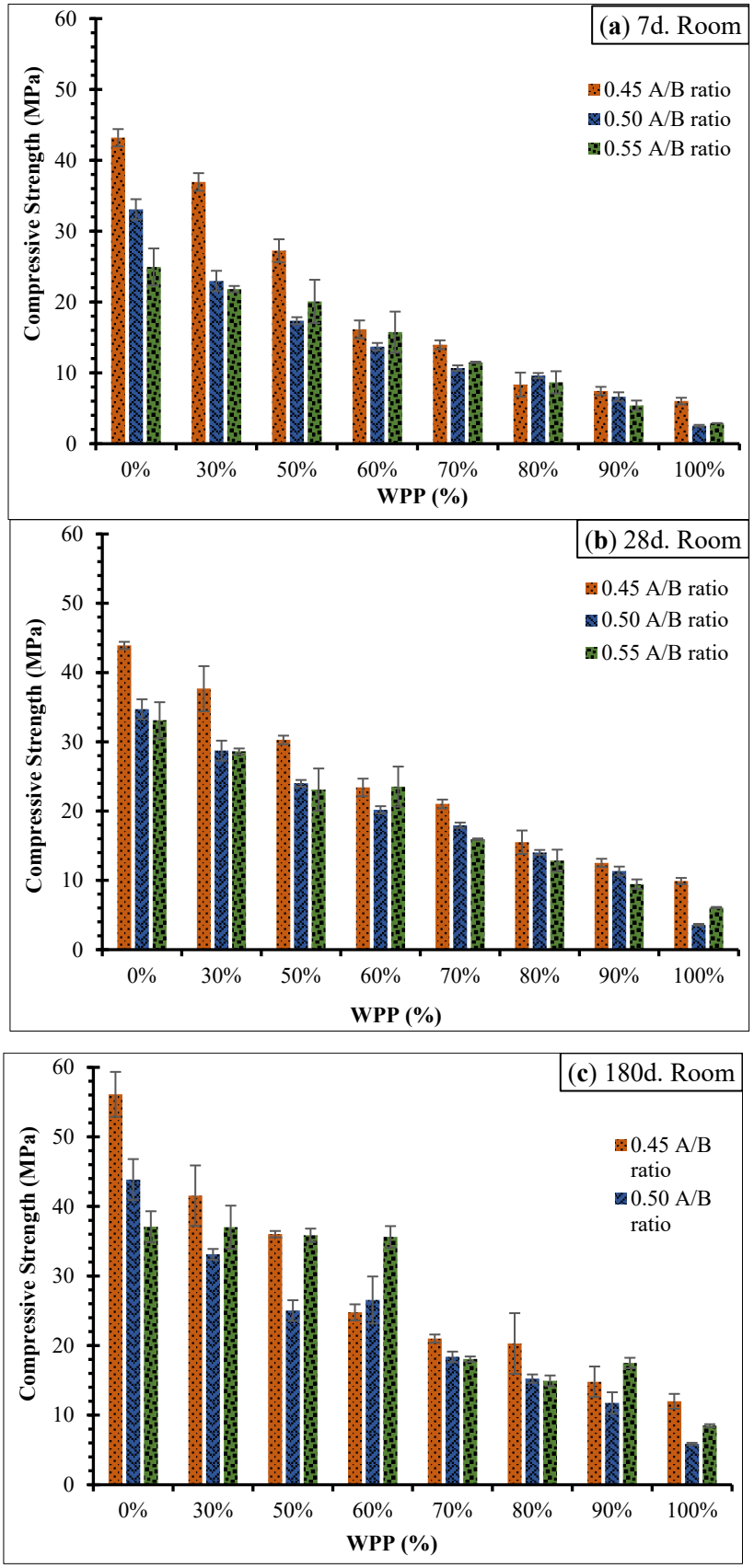

Figure 6. Compressive strength of GC mixes cured at ambient temperature for (**a**) 7 days, (**b**) 28 days, and (**c**) 180 days.

As demonstrated in Figure 6, there is an obvious difference between different A/B ratios of slag geopolymer composites that do not contain WPP. The compressive strength reduces sharply from 60.86 MPa to 37.27 MPa due to an increase in the A/B ratio from 0.45 to 0.55, respectively. A similar trend was observed for GGBFS-based geopolymers; the maximal compressive strength was achieved with an optimal A/B ratio of 0.45 [75]. Higher compressive strength values obtained with a lower A/B ratio of 0.45 may be attributed to a superior ability to dissolve the precursors based on WPP/GGBFS and build a polymerized network with a stronger bond with the precursor particles that have dissolved. However, increases in the A/B ratio cause a decrease in compressive strength, which is related to silica coagulation and faster setting. This also results in electrostatic shielding, which decreases ion activity and prevents precursors from dissolving, hence reducing compressive strength [76]. The compressive strength of combined fly ash/slag-based GC is significantly impacted by a higher A/B ratio at an early age. Still, this elevated ratio has a slight impact on the same concrete's compressive strength at a later age [77].

Effect of WPP Content

The use of different precursors (WPP and GGBFS) in the manufacturing of GC resulted in various compressive strength results, as presented in Figure 7. Overall, geopolymers made with 100% WPP as a precursor provided the lowest results. In contrast, geopolymers produced with 100% GGBFS as a precursor showed the maximum compressive strength despite several discrepancies observed according to other mixture parameters. The presence of pores and the non-active cement particles that were left unreacted after the completion of the geopolymerization reaction may be behind the decrease in the compressive strength of the GC. The compressive strength decreases in the order of (M45–0% (60.86 MPa) > M45–50% (42.17 MPa) > M45–90% (17.35 MPa)) at 28 days of 60 °C of heat (Figures 8 and 9). Additionally, the substantial drops in compressive strength may show how incorporating WPP into the synthesis mixes has an adverse effect. This could be because of the reactive characteristics of each of its components, which may not have contributed sufficiently to the system's enough level of geopolymerization. However, the compressive strength results of GC produced with 70% of WPP precursors of 28.37 MPa at 28 days subsequent curing at a temperature of 60 °C for 24 h is considered applicable for many of the structural applications of concrete, such as structural precast members, bearing blocks and bricks. It is possible to assess the geopolymerization reactions of precursors in geopolymer products with respect to various source materials in terms of their solubility, fineness, particle size distribution, amorphousness degree, and chemical composition [78,79]. Precursors with higher concentrations of siliceous/aluminous oxides, smaller particle sizes, and more prominent amorphous structures are typically thought to be geopolymerized more efficiently [80]. In the current work, WPP and GGBFS were used as the coarse-size precursors. However, the precursors' chemical compositions are similar, and the compressive strength value differences in WPP and GGBFS may be attributed to these precursors' differing zeta potential [81]. An increased Si/Al ratio may cause the formation of aluminum–silicate compounds with lower strengths due to less cross-linking, and even very slight changes in Si and Al contents can have a substantial influence on the characteristics of GCs [82]. The main distinguishing factors between WPP and GGBFS precursors are the considerably higher SiO_2 content (45.84%) and lower Al_2O_3 content (10.24%) of WPP. Its CaO (31.94%) contents are also higher, but Na2O (0.05%) is lower. The substantially higher Si/Al ratio in geopolymers may potentially be connected to the decreases in compressive strength values. It might also have occurred because excess calcium hydroxide was applied to the un-hydrated cement. Consequently, an ineffective hydration process may cause the strength properties of the GC to deteriorate.

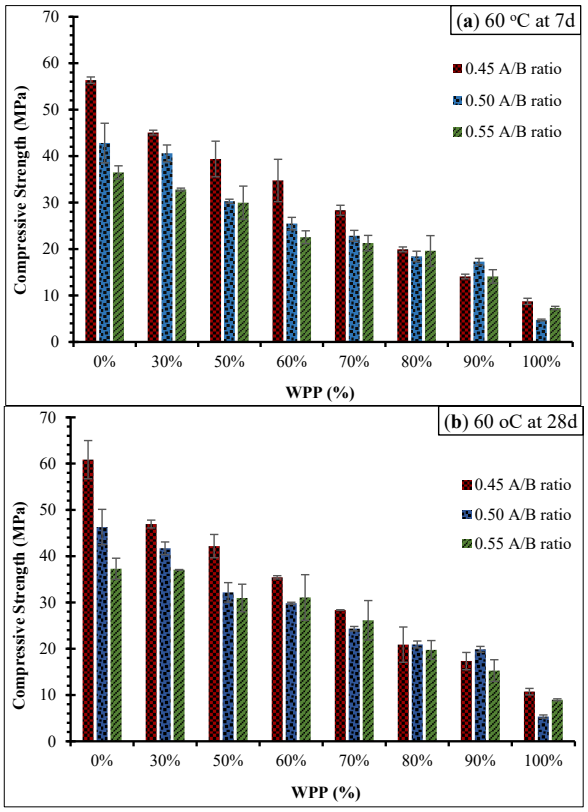

Figure 7. The compressive strength of GPC mixes cured at a 60 °C oven curing temperature for (**a**) 7 days and (**b**) 28 days.

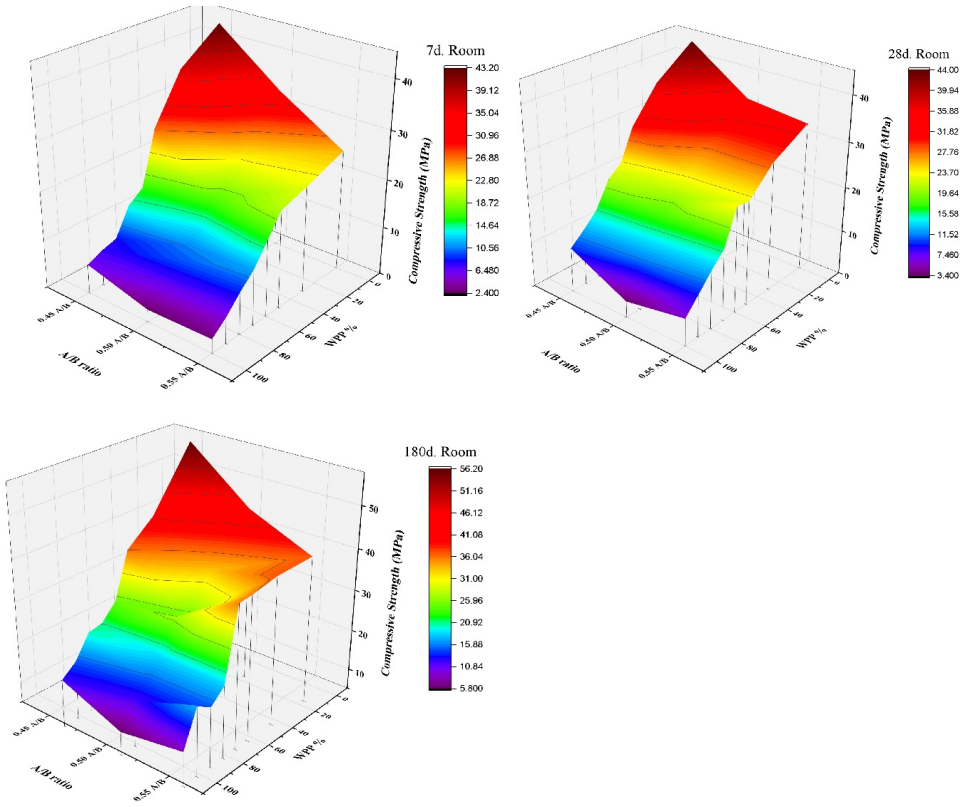

Figure 8. Influence of WPP% content on compressive strength of GC cured at ambient temperature for 7, 28, and 180 days.

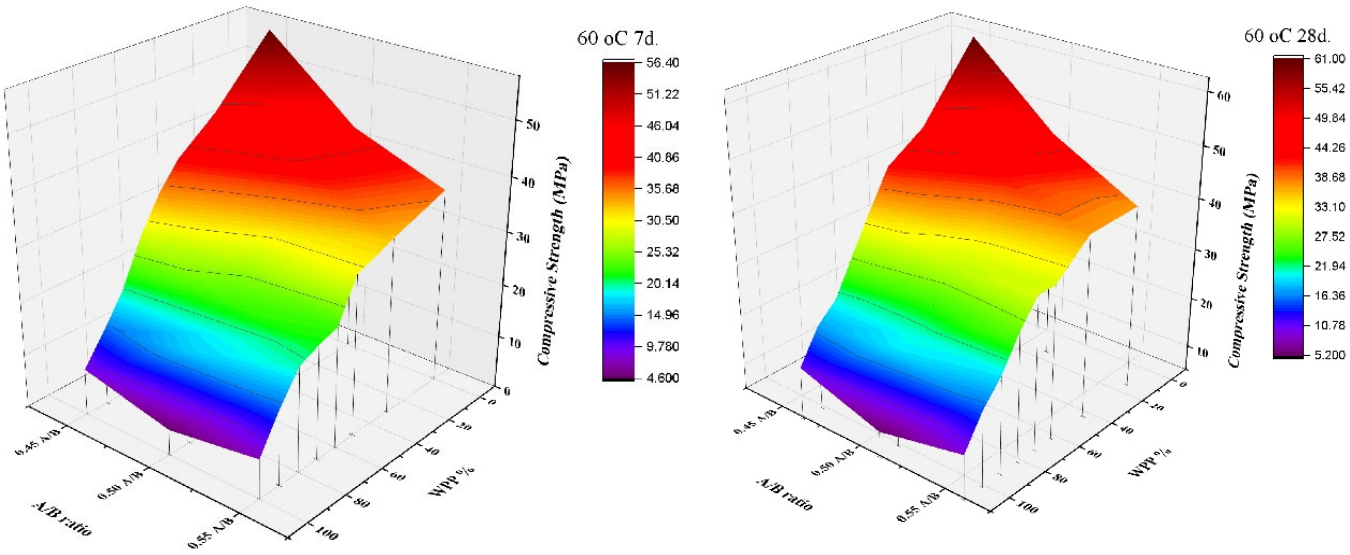

Figure 9. Influence of WPP% content on compressive strength of GC in 7, 28, and 180 days and cured at 60 °C temperature for 24 h.

Additionally, it is observed that when CaO consumes NaOH, the compressive strength results drop with greater CaO amounts [51]. Additionally, a different study concluded that pumice powder (PP) with considerably high amorphous silica contents could assist in producing cementitious geopolymer gels by encouraging the development of strength through the use of alumina present in the geopolymer system [83]. Furthermore, the greater the WPP/GGBFS content, the more advantageous the increase in compressive strength, since GGBFS has a larger calcium ion concentration than WPP. Moreover, GGFBS particles exhibit a high degree of geopolymerization due to their highly reactive surface. Furthermore, one of the most significant aspects to consider in determining the strength of the GC is the A/B [84].

3.2.3. Effect of Curing Condition

According to the outcomes of the research that was conducted, the relation between the age, curing temperature, and compressive strength of concrete made using WPP/GGBFS is displayed in Figure 10. The time and temperature of the curing process are critical factors that influence the compressive strength increase in GC [75]. The maximum compressive strength was achieved when GGFBS was fully utilized as a precursor in GC. Age evidently has an impact on compressive strength. The 7-day, 28-day, and 180-day compressive strengths of the GC mixture with GGBFS are (43.19) MPa, (43.92) MPa, and (56.12) MPa, respectively, at ambient temperature. However, the compressive strengths of the GC mixture with 50% of WPP are (27.92) MPa, (31.43) MPa, and (35.71) MPa, respectively, at the same age and curing condition, which is more than the compressive strength requirement of structural concrete. The potential to produce GC cured at ambient temperature or thermal curing without sacrificing its mechanical qualities would reduce the amount of energy used in the manufacturing of GC and enable its usage in both precast concrete and cast-in-situ applications.

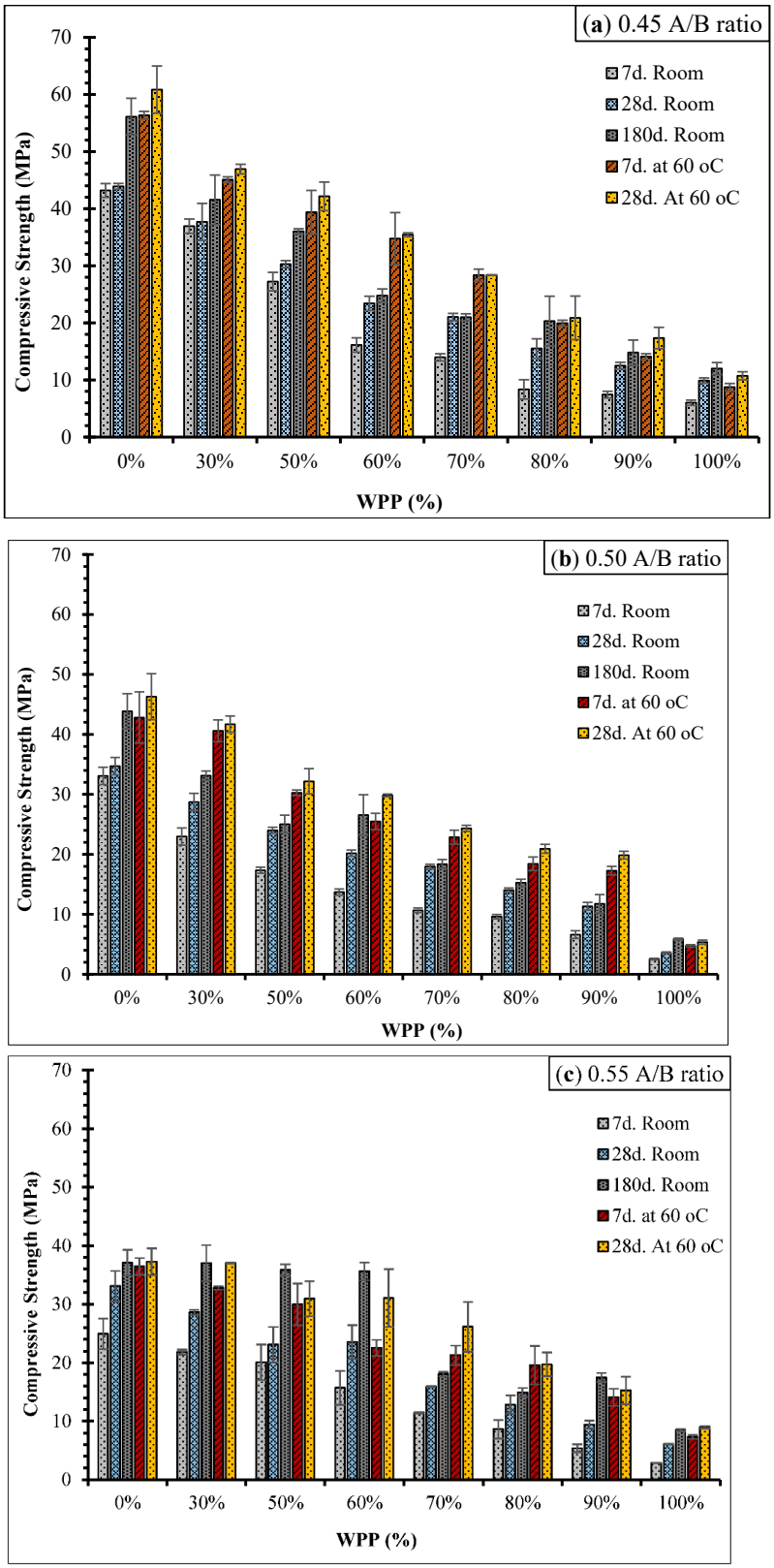

Figure 10. The influence of WPP % content on the compressive strength of GC cured at ambient temperature for 7, 28, and 180 days and oven curing for 7 and 28 days [(**a**) A/B ratio: 0.45, (**b**) A/B ratio: 0.50, and (**c**) A/B ratio: 0.55].

Geopolymer composites are significantly influenced by curing temperature. According to Figure 10, which indicates the influence of ambient and heat curing on the result of

compressive strength, it has been reported that as the temperature of the curing process increases from room temperature to 60 °C for 24 h, the compressive strength is enhanced. At 60 °C, the compressive strength is at its highest. The fundamental reason for this is that a rise in temperature accelerates the ground polymerization process by accelerating the rate at which WPP and GGBFS particles dissolve and hydrate. Concurrently, the rise in temperature promotes the removal of water and acceleration of the gel phase's formation [85]. However, the findings reported that although the compressive strength of GC initially enhances rapidly before stabilizing with age, the geopolymerization reaction is frequently finished in the initial seven days. The results are in line with those published in the literature; as the age of geopolymer increases, the strength continues to increase [86]. Several efforts have been made to investigate the influences of ambient curing on GC, and a number of remarkable studies have provided information regarding its properties. The findings of this investigation showed that samples that were cured at room temperature gradually increased in compressive strength over time. In contrast, samples that were cured in an oven showed fewer changes in strength. The findings demonstrated that, in comparison to ambient curing conditions, the external exposure of the geopolymer concrete to heat curing led to a more considerable development in compressive strength. It was found that when the geopolymer was cured under ambient conditions, the silicon and aluminum ions gradually dissolved and that heat curing improved the mechanical characteristics [87]. For GC, oven curing conditions have been used in most investigations rather than ambient curing. Increased polymerization was achieved by extending the curing period, which increased compressive strength. The curing procedure can take up to 24 h, and the strength rate development was significant; after that, it increased more slowly [88]. According to the previous findings, concrete's early age strength was mostly attributable to the GGBFS [89]. The compressive strength of GC specimens after 28 days at 60 °C heat curing was greater than that of OPC specimens and GC treated at standard temperatures. According to research by Hardjito (2005) [90], compressive strength is enhanced by raising the oven curing temperature. However, at the 60 °C curing temperature threshold, this rise loss is significant. The advantages of raising the curing temperature do have a limit. Concrete may start to weaken and deteriorate if the temperature reaches too high [88]. Therefore, in order to attain optimum strength, it is crucial to determine the ideal temperature for curing a certain mix design.

3.2.4. Flexural Tensile Strength

The analysis of the results for the flexural tensile strength of the geopolymer concretes is illustrated in Figure 11. This figure illustrates the evolution of the flexural tensile strength with different A/B ratios and WPP content at 180 days of ambient curing. It is observed that the flexural strength drops as the ratio of A/B increases. The flexural strengths of M45–0%, M50–0%, and M55–0% samples are 4.96 MPa, 4.11 MPa, and 3.95 MPa, respectively, after 180 days under ambient temperature. The flexural strength of the GC decreases in a way similar to that of the GC specimens under compression as the dosage of the A/B ratio is decreased. As a result, the geopolymer samples' trend and compressive strength are comparable [77]. The geopolymer concrete with 0.45 A/B ratio with GGBFS alone and cured under 60 °C for 24 h had the highest flexural strength than the samples with 0.55 A/B ratio with the same condition and cured under ambient temperature. As shown in Figure 11, the flexural strengths of M45–100%, M45–80%, M45–50%, M45–30%, and M45–0% samples are 4.04 MPa, 4.20 MPa, 4.23 MPa, 4.33 MPa, 4.96 MPa, respectively, after 180 days of ambient curing.

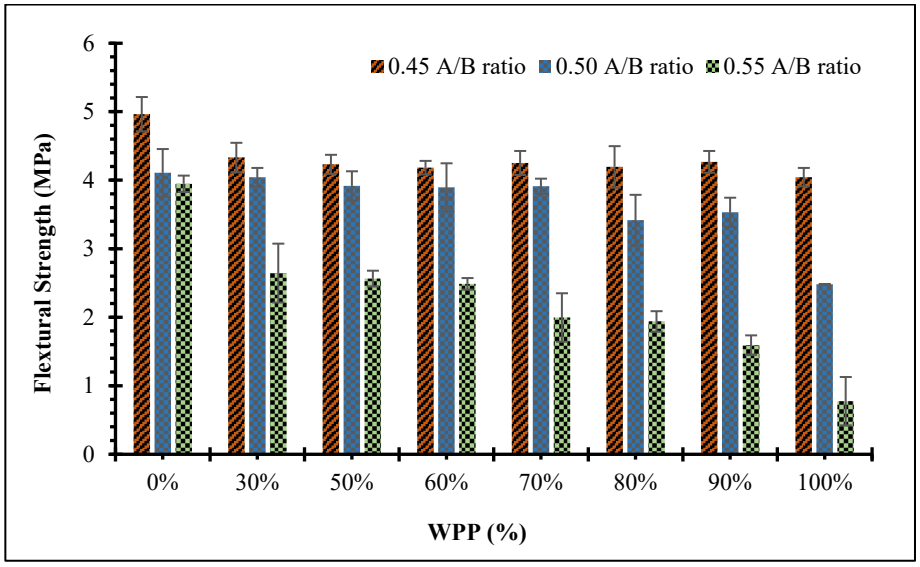

Figure 11. Flexural strength of GC mixes cured at ambient temperature for 28 days.

According to Figure 11, when WPP content is employed in amounts from 90 to 0% with 0.45 A/B, the flexural strength declines from 4.96 MPa to 4.04 MPa, respectively. The highest flexural strength is attained with a mix with a 100% dosage of the GGBFS.

Similar results were reported for decreasing the tensile strength of GC mixes because of the incorporation of a small amount of WPP. Utilizing a lower substitute amount of WPP in GC resulted in a decrease in the A/B ratio, as well as an improvement in the mortar matrix and the interfacial transition zone. However, with increasing the WPP content, the flexural strength decreases; this might be due to the inhomogeneity in uncured resin zones. When additional WPP was added to the geopolymer concrete, this zone became the weakest one, where cracks were able to propagate through the coarse aggregate particles.

3.2.5. Ultrasonic Pulse Velocity and Compressive Strength Correlation

The UPV values of the GC mixes with different A/B ratio and WPP content cured at ambient temperature for 180 days were correlated with the values of the compressive strength of those mixes. Figure 12 demonstrates the correlation. A linear equation (Equation (1)) is expected to depict the correlation between the UPV and compressive strength values of every GC specimen. The data points for compressive strength and UPV show a strong correlation (R^2 = 0.95), according to the correlation coefficients.

$$\text{Compressive strength} = 0.0289(\text{UPV}) - 79.995 \quad (1)$$

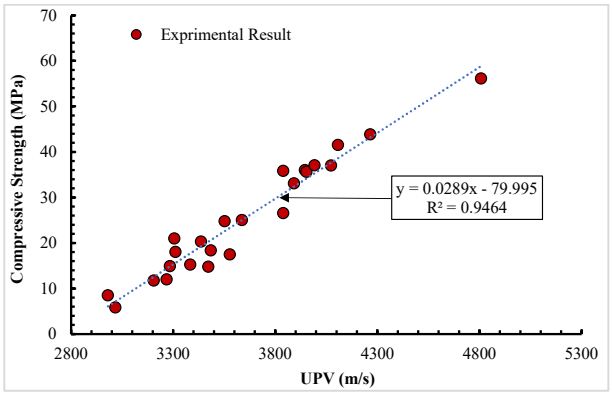

Figure 12. The correlation between 180-day compressive strength for GC mixes (different A/B ratio and WPP%) and UPV values.

3.3. Water Absorption

A number of different parameters, such as the binder type as well as the A/B ratio, can influence the water absorption properties of GC. Generally, the water absorption of GC is lower compared to OPC concrete. This is mostly because of its denser microstructure, which is enhanced by a larger concentration of aluminosilicate gel. The water absorption results for the GC mixes made with varying A/B ratios are displayed in Figure 13. The figure demonstrates that the mixes with the higher A/B ratio exhibited higher water absorption.

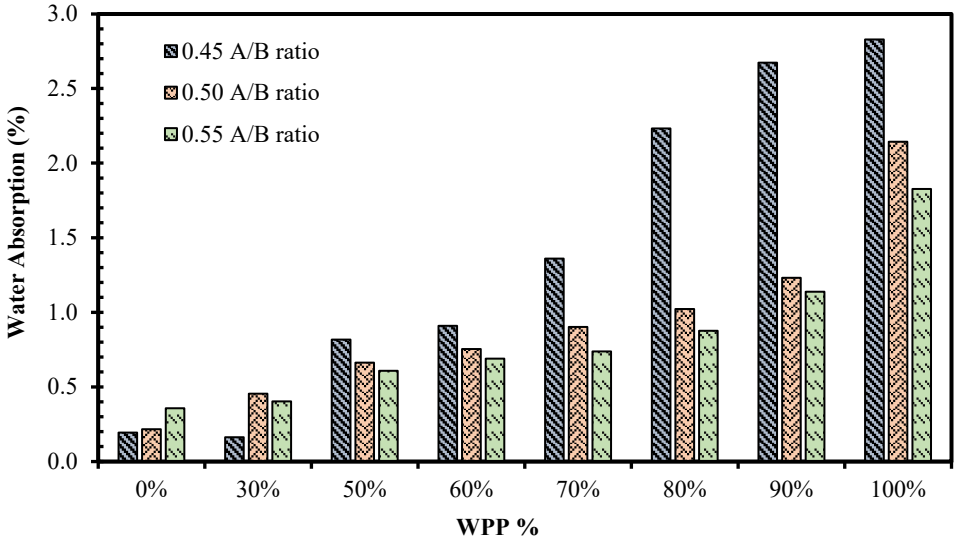

Figure 13. Water absorption of ambient-cured geopolymer concrete at 180 days under ambient temperature (A/B ratio: 0.45, 0.50 and 0.55).

GC samples with an A/B ratio of 0.45 reported substantially higher values of water absorption in comparison to those with ratios of 0.5 and 0.55. It has been shown that the A/B ratio has a significant impact on the water absorption of GC. According to [91], geopolymer concrete mixes exhibited lower pore volume characteristics and better absorption compared to ordinary concrete. Excess water can be added to concrete to make it more workable, but it eventually evaporates and leaves pores behind [92]. One important determinant of a concrete construction's durability is its water absorption coefficient. Mixes with only a GGFBS binder showed lower water absorption than mixes with both WPP and GGFBS. Increasing the WPP replacement level from 0 to 100% also resulted in an increase in water absorption, by 2.62%. Increasing the GGFBS content may lead to the creation of cracks in the GC mix matrix that open capillary channels for water penetration.

3.4. Microstructure Analysis

The building materials' microstructure is usually investigated by a microstructural assessment that includes the interpretation of microstructure imaging. In this work, SEM images were taken for the prepared geopolymer concrete samples. Typical SEM images for the GC based on 100% GGBFS and (50% WPP plus 50% WPP) prepared using a 0.45 alkaline activator/binder ratio are shown in Figure 14. The GC mixes based on 100% GGBFS (Figure 14a) were observed to have a tightly packed, well-compacted, and dense microstructure. The GGBFS content seemed to activate the polymerization process highly. It aided in the dissolution of more silicate and aluminate species, which contributed to the formation of extra Ca-Al-Si gel in the GC paste. However, tiny microcracks were observed in the GC matrix resulting from the evaporation of water used in the preparation of the alkaline activator during the heat curing of the samples. The incorporation of WPP in GC mixes showed a less compacted and less homogeneous structure matrix when compared to the GC based on 100% GGBFS cured pastes. The morphology of the tested samples reflected

the reason for the decline in compressive strength of the samples incorporated with WPP compared to those that had 100% GGBFS content.

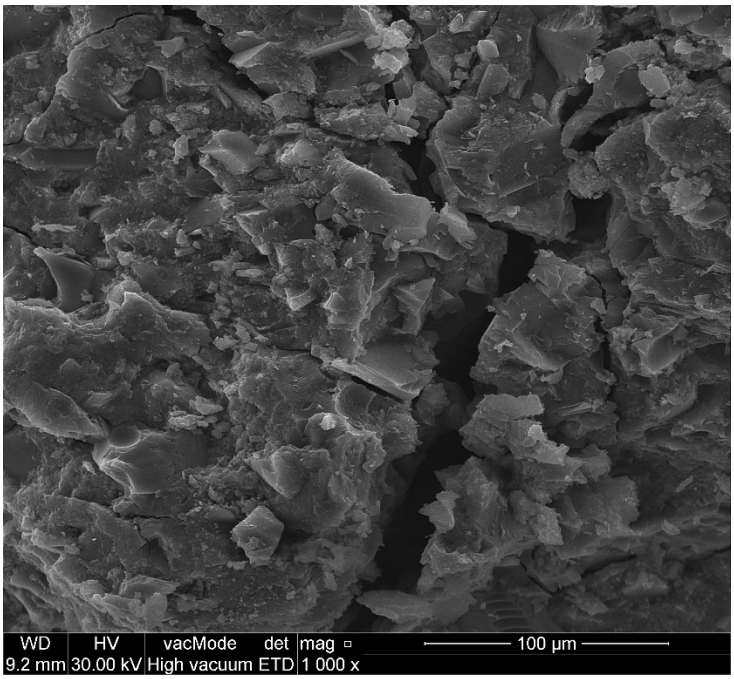

(**a**) 0.45 A/B with 0% of WPP

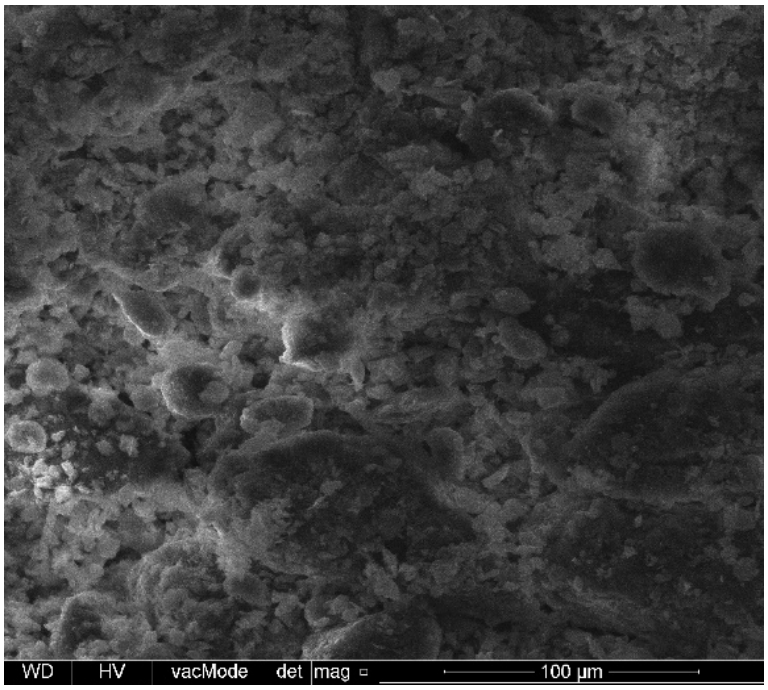

(**b**) 0.45 A/B with 50% of WPP

Figure 14. The SEM images of geopolymer concrete samples for (**a**) 0.45 A/B ratio with 0% of WPP and (**b**) 0.45 A/B with 50% of WPP.

4. Conclusions

This study investigated the feasibility of using waste pumice powder as a precursor in place of granular blast-furnace slag to manufacture geopolymer concrete and study the effect of WPP and A/B ratio on the fresh, mechanical, physical, and microstructure properties of slag-based geopolymer. The results revealed that replacing slag with WPP

at a content of 50% can result in a geopolymer concrete with good performance that is appropriate for use in various structural applications. A potential and promising GC system can be prepared from a combination of waste pumice powder (WPP) and GGFBS. A summary of the conclusions drawn from the current work is shown below:

1. A decrease in A/B ratios leads to a longer setting process. The initial setting time of the GC (M45–100%) is (153 min) while the initial setting time of M50–100% is (96 min). Setting times decrease with increased alkali activator content. However, the higher WPP content led to extended setting times (both the initial and final). With an increase in the content of GGBFS, there is a notable decrease in the setting time.
2. The incorporation of GGBFS with WPP decreases the workability and strength of GC due to the irregular shape of WPP reduces its fluidity, which affects the workability and flowability of fresh geopolymer concrete.
3. The ratio of alkaline to binder in GC plays a crucial role in GC strength (compressive and flexural). The optimum strength of 60.86 MPa was obtained using the 0.45 A/B ratio and 0% of WPP at 28 days with 60 °C curing for 24 h. High A/B ratios result in lower compressive strength.
4. The geopolymerization reaction is accelerated with heat curing temperatures (60 °C). However, a high-strength geopolymer with 56.11 MPa can be obtained without heat curing when subjected to 180 days of an ambient curing temperature.
5. Slag-based geopolymer concrete has a lower water absorption compared to the GC that contains WPP. Increasing the WPP replacement level from 0 to 100% also resulted in an increase in water absorption, with 2.62%. Increasing the GGFBS content may lead to the creation of cracks in the GC mix matrix that open capillary channels for water penetration.
6. The replacement of WPP with GGBFS in geopolymer concrete up to 70% using heat curing at 60 °C is applicable for various structural applications of concrete.
7. Overall, the results showed that geopolymer mixes up to 70% of WPP with 60 °C of heat curing for 24 h could satisfy different requirements of structural applications of building materials, such as structural precast members, bearing blocks, and bricks. The good strength performance, lower water absorption, and use of waste precursors as binders instead of cement in normal concrete decrease the carbon footprint and environmental pollution resulting from the cement industry and building construction.

Author Contributions: All authors contributed to the conception and design. The literature review was carried out by Z.S. The first draft of the manuscript was written by Z.S. The article was revised by K.H.Y. and I.K. The supervision was done by K.H.Y. and I.K. All authors have read and agreed to the published version of the manuscript.

Funding: This research received no external funding.

Data Availability Statement: The data supporting the conclusions of this article are included with the article.

Acknowledgments: The authors wish to thank the technical staff of the Materials Laboratory of Soran University and Erbil Construction Laboratory (ECL), Kurdistan, Iraq.

Conflicts of Interest: The authors declare no conflicts of interest.

References

1. Xu, J.H.; Fleiter, T.; Eichhammer, W.; Fan, Y. Energy consumption and CO_2 emissions in China's cement industry: A perspective from LMDI decomposition analysis. *Energy Policy* **2012**, *50*, 821–832. [CrossRef]
2. Cao, Z.; Shen, L.; Liu, L.; Zhong, S. Analysis on major drivers of cement consumption during the urbanization process in China. *J. Clean. Prod.* **2016**, *133*, 304–313. [CrossRef]
3. Rasheed, R.; Tahir, F.; Afzaal, M.; Ahmad, S.R. Decomposition analytics of carbon emissions by cement manufacturing—A way forward towards carbon neutrality in a developing country. *Environ. Sci. Pollut. Res.* **2022**, *29*, 49429–49438. [CrossRef]
4. Afkhami, B.; Akbarian, B.; Beheshti, A.N.; Kakaee, A.H.; Shabani, B. Energy consumption assessment in a cement production plant. *Sustain. Energy Technol. Assess.* **2015**, *10*, 84–89. [CrossRef]

5. Hanifa, M.; Agarwal, R.; Sharma, U.; Thapliyal, P.C.; Singh, L.P. A review on CO_2 capture and sequestration in the construction industry: Emerging approaches and commercialised technologies. *J. CO_2 Util.* **2023**, *67*, 102292. [CrossRef]
6. Gale, J.; Mahasenan, N.; Smith, S.; Humphreys, K. The Cement Industry and Global Climate Change: Current and Potential Future Cement Industry CO_2 Emissions. In *Greenhouse Gas Control Technologies, Proceedings of the 6th International Conference on Greenhouse Gas Control Technologies, Kyoto, Japan, 1–4 October 2002*; Elsevier: Amsterdam, The Netherlands, 2003; Volume II, pp. 995–1000.
7. Fennell, P.S.; Davis, S.J.; Mohammed, A. Decarbonizing cement production. *Joule* **2021**, *5*, 1305–1311. [CrossRef]
8. Salas, D.A.; Ramirez, A.D.; Rodríguez, C.R.; Petroche, D.M.; Boero, A.J.; Duque-Rivera, J. Environmental impacts, life cycle assessment and potential improvement measures for cement production: A literature review. *J. Clean. Prod.* **2016**, *113*, 114–122. [CrossRef]
9. Zhang, Z.; Lin, B. Energy Conservation and Emission Reduction of Chinese Cement Industry: From a Perspective of Factor Substitutions. *Emerg. Mark. Financ. Trade* **2019**, *55*, 967–979. [CrossRef]
10. Kajaste, R.; Hurme, M. Cement industry greenhouse gas emissions—Management options and abatement cost. *J. Clean. Prod.* **2016**, *112*, 4041–4052. [CrossRef]
11. Singh, N.B.; Middendorf, B. Geopolymers as an alternative to Portland cement: An overview. *Constr. Build. Mater.* **2020**, *237*, 117455. [CrossRef]
12. Wu, Y.; Lu, B.; Bai, T.; Wang, H.; Du, F.; Zhang, Y.; Cai, L.; Jiang, C.; Wang, W. Geopolymer, green alkali activated cementitious material: Synthesis, applications and challenges. *Constr. Build. Mater.* **2019**, *224*, 930–949. [CrossRef]
13. Zakka, W.P.; Abdul Shukor Lim, N.H.; Chau Khun, M. A scientometric review of geopolymer concrete. *J. Clean. Prod.* **2021**, *280*, 124353. [CrossRef]
14. Van Deventer, J.S.J.; Provis, J.L.; Duxson, P.; Brice, D.G. Chemical research and climate change as drivers in the commercial adoption of alkali activated materials. *Waste Biomass Valorization* **2010**, *1*, 145–155. [CrossRef]
15. Ma, C.K.; Awang, A.Z.; Omar, W. Structural and material performance of geopolymer concrete: A review. *Constr. Build. Mater.* **2018**, *186*, 90–102. [CrossRef]
16. Nguyen, K.T.; Ahn, N.; Le, T.A.; Lee, K. Theoretical and experimental study on mechanical properties and flexural strength of fly ash-geopolymer concrete. *Constr. Build. Mater.* **2016**, *106*, 65–77. [CrossRef]
17. Chowdhury, S.; Mohapatra, S.; Gaur, A.; Dwivedi, G.; Soni, A. Study of various properties of geopolymer concrete—A review. *Mater. Today Proc.* **2020**, *46*, 5687–5695. [CrossRef]
18. Divvala, S.; Rani, M.S. Early strength properties of geopolymer concrete composites: An experimental study. *Mater. Today Proc.* **2021**, *47*, 3770–3777. [CrossRef]
19. Nnaemeka, O.F.; Singh, N.B. Durability properties of geopolymer concrete made from fly ash in presence of Kaolin. *Mater. Today Proc.* **2019**, *29*, 781–784. [CrossRef]
20. Albitar, M.; Mohamed Ali, M.S.; Visintin, P.; Drechsler, M. Durability evaluation of geopolymer and conventional concretes. *Constr. Build. Mater.* **2017**, *136*, 374–385. [CrossRef]
21. Amran, M.; Al-Fakih, A.; Chu, S.H.; Fediuk, R.; Haruna, S.; Azevedo, A.; Vatin, N. Long-term durability properties of geopolymer concrete: An in-depth review. *Case Stud. Constr. Mater.* **2021**, *15*, e00661. [CrossRef]
22. Valencia Saavedra, W.G.; Mejía de Gutiérrez, R. Performance of geopolymer concrete composed of fly ash after exposure to elevated temperatures. *Constr. Build. Mater.* **2017**, *154*, 229–235. [CrossRef]
23. Wasim, M.; Ngo, T.D.; Law, D. A state-of-the-art review on the durability of geopolymer concrete for sustainable structures and infrastructure. *Constr. Build. Mater.* **2021**, *291*, 123381. [CrossRef]
24. Kumar, L.M.; Revathi, V. Durability studies in alkaline activated systems (metakaolin-bottom ash): A prospective study. *Bol. la Soc. Esp. Ceram. y Vidr.* **2023**, *62*, 40–55. [CrossRef]
25. Ariffin, M.A.M.; Bhutta, M.A.R.; Hussin, M.W.; Mohd Tahir, M.; Aziah, N. Sulfuric acid resistance of blended ash geopolymer concrete. *Constr. Build. Mater.* **2013**, *43*, 80–86. [CrossRef]
26. Pacheco-Torgal, F.; Abdollahnejad, Z.; Camões, A.F.; Jamshidi, M.; Ding, Y. Durability of alkali-activated binders: A clear advantage over Portland cement or an unproven issue? *Constr. Build. Mater.* **2012**, *30*, 400–405. [CrossRef]
27. Ryu, G.S.; Lee, Y.B.; Koh, K.T.; Chung, Y.S. The mechanical properties of fly ash-based geopolymer concrete with alkaline activators. *Constr. Build. Mater.* **2013**, *47*, 409–418. [CrossRef]
28. Meesala, C.R.; Verma, N.K.; Kumar, S. Critical review on fly-ash based geopolymer concrete. *Struct. Concr.* **2020**, *21*, 1013–1028. [CrossRef]
29. Ali, A.; uz Zaman Khan, Q.; Saqib Mehboob, S.; Tayyab, A.; Hayyat, K.; Khan, D.; Ul Haq, I.; Bux alias Imran Latif Qureshi, Q. Enhancing multi-objective mix design for GGBS-based geopolymer concrete with natural mineral blends under ambient curing: A Taguchi-Grey relational optimization. *Ain Shams Eng. J.* **2024**, *15*, 102708. [CrossRef]
30. Reddy, M.S.; Dinakar, P.; Rao, B.H. Mix design development of fly ash and ground granulated blast furnace slag based geopolymer concrete. *J. Build. Eng.* **2018**, *20*, 712–722. [CrossRef]
31. Albidah, A.; Alghannam, M.; Abbas, H.; Almusallam, T.; Al-Salloum, Y. Characteristics of metakaolin-based geopolymer concrete for different mix design parameters. *J. Mater. Res. Technol.* **2021**, *10*, 84–98. [CrossRef]
32. Gupta, A.; Gupta, N.; Saxena, K.K. Experimental study of the mechanical and durability properties of Slag and Calcined Clay based geopolymer composite. *Adv. Mater. Process. Technol.* **2022**, *8*, 655–669. [CrossRef]

33. Singh, S.; Maiti, S.; Bisht, R.S.; Panigrahi, S.K.; Yadav, S. Large CO_2 reduction and enhanced thermal performance of agro-forestry, construction and demolition waste based fly ash bricks for sustainable construction. *Sci. Rep.* **2024**, *14*, 8368. [CrossRef]
34. Khalifa, A.Z.; Cizer, Ö.; Pontikes, Y.; Heath, A.; Patureau, P.; Bernal, S.A.; Marsh, A.T.M. Advances in alkali-activation of clay minerals. *Cem. Concr. Res.* **2020**, *132*, 106050. [CrossRef]
35. Rashad, A.M.; Sadek, D.M. An investigation on Portland cement replaced by high-volume GGBS pastes modified with micro-sized metakaolin subjected to elevated temperatures. *Int. J. Sustain. Built Environ.* **2017**, *6*, 91–101. [CrossRef]
36. Elavarasan, S.; Priya, A.K.; Ajai, N.; Akash, S.; Annie, T.J.; Bhuvana, G. Experimental study on partial replacement of cement by metakaolin and GGBS. *Mater. Today Proc.* **2020**, *37*, 3527–3530. [CrossRef]
37. Xie, T.; Visintin, P.; Zhao, X.; Gravina, R. Mix design and mechanical properties of geopolymer and alkali activated concrete: Review of the state-of-the-art and the development of a new unified approach. *Constr. Build. Mater.* **2020**, *256*, 119380. [CrossRef]
38. Chiranjeevi, K.; Abraham, M.; Rath, B.; Praveenkumar, T.R. Enhancing the properties of geopolymer concrete using nano-silica and microstructure assessment: A sustainable approach. *Sci. Rep.* **2023**, *13*, 17302. [CrossRef]
39. Zeyad, A.M.; Magbool, H.M.; Tayeh, B.A.; Garcez de Azevedo, A.R.; Abutaleb, A.; Hussain, Q. Production of geopolymer concrete by utilizing volcanic pumice dust. *Case Stud. Constr. Mater.* **2022**, *16*, e00802. [CrossRef]
40. Szabó, R.; Kristály, F.; Nagy, S.; Singla, R.; Mucsi, G.; Kumar, S. Reaction, structure and properties of eco-friendly geopolymer cement derived from mechanically activated pumice. *Ceram. Int.* **2023**, *49*, 6756–6763. [CrossRef]
41. Bagci, C.; Kafkas, D.; Samuel, D.M.; Kriven, W.M. Sustainable activation of pumice with partially variable substitutions of metakaolin and/or fumed silica. *Int. J. Appl. Ceram. Technol.* **2024**, *21*, 818–828. [CrossRef]
42. Oti, J.; Adeleke, B.O.; Anowie, F.X.; Kinuthia, J.M.; Ekwulo, E. Mechanical Properties of a Sustainable Low-Carbon Geopolymer Concrete Using a Pumice-Derived Sodium Silicate Solution. *Materials* **2024**, *17*, 1792. [CrossRef] [PubMed]
43. Talaat Mohammed, D.; Yaltay, N. Strength and elevated temperature resistance properties of the geopolymer paste produced with ground granulated blast furnace slag and pumice powder. *Ain Shams Eng. J.* **2024**, *15*, 102483. [CrossRef]
44. Bobirică, C.; Orbeci, C.; Bobirică, L.; Palade, P.; Deleanu, C.; Pantilimon, C.M.; Pîrvu, C.; Radu, I.C. Influence of red mud and waste glass on the microstructure, strength, and leaching behavior of bottom ash-based geopolymer composites. *Sci. Rep.* **2020**, *10*, 19827. [CrossRef] [PubMed]
45. Ahmed, J.K.; Atmaca, N.; Khoshnaw, G.J. Building a sustainable future: An experimental study on recycled brick waste powder in engineered geopolymer composites. *Case Stud. Constr. Mater.* **2024**, *20*, e02863. [CrossRef]
46. Hwang, C.L.; Damtie Yehualaw, M.; Vo, D.H.; Huynh, T.P. Development of high-strength alkali-activated pastes containing high volumes of waste brick and ceramic powders. *Constr. Build. Mater.* **2019**, *218*, 519–529. [CrossRef]
47. Mahmoodi, O.; Siad, H.; Lachemi, M.; Dadsetan, S.; Sahmaran, M. Development and characterization of binary recycled ceramic tile and brick wastes-based geopolymers at ambient and high temperatures. *Constr. Build. Mater.* **2021**, *301*, 124138. [CrossRef]
48. Amin, S.K.; El-Sherbiny, S.A.; El-Magd, A.A.M.A.; Belal, A.; Abadir, M.F. Fabrication of geopolymer bricks using ceramic dust waste. *Constr. Build. Mater.* **2017**, *157*, 610–620. [CrossRef]
49. Kaya, M.; Köksal, F.; Bayram, M.; Nodehi, M.; Gencel, O.; Ozbakkaloglu, T. The effect of marble powder on physico-mechanical and microstructural properties of kaolin-based geopolymer pastes. *Struct. Concr.* **2023**, *24*, 6485–6504. [CrossRef]
50. Uysal, M.; Aygörmez, Y.; Canpolat, O.; Cosgun, T.; Faruk Kuranlı, Ö. Investigation of using waste marble powder, brick powder, ceramic powder, glass powder, and rice husk ash as eco-friendly aggregate in sustainable red mud-metakaolin based geopolymer composites. *Constr. Build. Mater.* **2022**, *361*, 129718. [CrossRef]
51. Komnitsas, K.; Zaharaki, D.; Vlachou, A.; Bartzas, G.; Galetakis, M. Effect of synthesis parameters on the quality of construction and demolition wastes (CDW) geopolymers. *Adv. Powder Technol.* **2015**, *26*, 368–376. [CrossRef]
52. Mahmoodi, O.; Siad, H.; Lachemi, M.; Sahmaran, M. Synthesis and optimization of binary systems of brick and concrete wastes geopolymers at ambient environment. *Constr. Build. Mater.* **2021**, *276*, 122217. [CrossRef]
53. Mahmoodi, O.; Siad, H.; Lachemi, M.; Dadsetan, S.; Sahmaran, M. Development of normal and very high strength geopolymer binders based on concrete waste at ambient environment. *J. Clean. Prod.* **2021**, *279*, 123436. [CrossRef]
54. Nath, P.; Sarker, P.K. Effect of GGBFS on setting, workability and early strength properties of fly ash geopolymer concrete cured in ambient condition. *Constr. Build. Mater.* **2014**, *66*, 163–171. [CrossRef]
55. ASTM. *Time of Setting of Hydraulic Cement by Vicat Needle 1*; ASTM International: West Conshohocken, PA, USA, 2004.
56. *ASTM C143/C143M*; Standard Test Method for Slump of Hydraulic-Cement Concrete. ASTM International: West Conshohocken, PA, USA, 2012.
57. *BS EN 12390-3:2001*; Testing Hardened Concrete—Part 3: Compressive Strength of Test Specimens. Scientific Research: Atlanta, GA, USA, 2002; pp. 4–10.
58. *ASTM D6272*; Standard Test Method for Flexural Properties of Unreinforced and Reinforced Plastics and Electrical Insulating Materials by Four-Point Bending. ASTM International: West Conshohocken, PA, USA, 2020. [CrossRef]
59. *ASTM C642*; Standard Test Method for Density, Absorption, and Voids in Hardened Concrete. ASTM International: West Conshohocken, PA, USA, 2021.
60. Tchadjie, L.N.; Ekolu, S.O. Enhancing the reactivity of aluminosilicate materials toward geopolymer synthesis. *J. Mater. Sci.* **2018**, *53*, 4709–4733. [CrossRef]
61. Ukritnukun, S.; Koshy, P.; Rawal, A.; Castel, A.; Sorrell, C.C. Predictive model of setting times and compressive strengths for low-alkali, ambient-cured, fly ash/slag-based geopolymers. *Minerals* **2020**, *10*, 920. [CrossRef]

62. Yusslee, E.; Beskhyroun, S. The potential of one-part alkali-activated materials (AAMs) as a concrete patch mortar. *Sci. Rep.* **2022**, *12*, 15902. [CrossRef]
63. Chindaprasirt, P.; De Silva, P.; Sagoe-Crentsil, K.; Hanjitsuwan, S. Effect of SiO_2 and Al_2O_2 on the setting and hardening of high calcium fly ash-based geopolymer systems. *J. Mater. Sci.* **2012**, *47*, 4876–4883. [CrossRef]
64. Qaidi, S.; Najm, H.M.; Abed, S.M.; Ahmed, H.U.; Al Dughaishi, H.; Al Lawati, J.; Sabri, M.M.; Alkhatib, F.; Milad, A. Fly Ash-Based Geopolymer Composites: A Review of the Compressive Strength and Microstructure Analysis. *Materials* **2022**, *15*, 7098. [CrossRef]
65. de Hita, M.J.; Criado, M. Influence of superplasticizers on the workability and mechanical development of binary and ternary blended cement and alkali-activated cement. *Constr. Build. Mater.* **2023**, *366*, 130272. [CrossRef]
66. Gugulothu, V.; Gunneswara Rao, T.D. Effect of Binder Content and Solution/Binder Ratio on Alkali-Activated Slag Concrete Activated with Neutral Grade Water Glass. *Arab. J. Sci. Eng.* **2020**, *45*, 8187–8197. [CrossRef]
67. Cherki El Idrissi, A.; Roziere, E.; Loukili, A.; Darson, S. Design of geopolymer grouts: The effects of water content and mineral precursor. *Eur. J. Environ. Civ. Eng.* **2018**, *22*, 628–649. [CrossRef]
68. Aliabdo, A.A.; Abd Elmoaty, A.E.M.; Salem, H.A. Effect of water addition, plasticizer and alkaline solution constitution on fly ash based geopolymer concrete performance. *Constr. Build. Mater.* **2016**, *121*, 694–703. [CrossRef]
69. Yao, Z.; Luo, L.; Qin, Y.; Cheng, J.; Qu, C. Research on mix design and mechanical performances of MK-GGBFS based geopolymer pastes using central composite design method. *Sci. Rep.* **2024**, *14*, 9101. [CrossRef] [PubMed]
70. Kashani, A.; Ngo, T.D.; Mendis, P. The effects of precursors on rheology and self-compactness of geopolymer concrete. *Mag. Concr. Res.* **2019**, *71*, 557–566. [CrossRef]
71. Meko, B.; Ighalo, J.O.; Ofuyatan, O.M. Enhancement of self-compactability of fresh self-compacting concrete: A review. *Clean. Mater.* **2021**, *1*, 100019. [CrossRef]
72. Ekmen, Ş.; Mermerdaş, K.; Algın, Z. Effect of oxide composition and ingredient proportions on the rheological and mechanical properties of geopolymer mortar incorporating pumice aggregate. *J. Build. Eng.* **2021**, *34*, 101893. [CrossRef]
73. Ng, C.; Alengaram, U.J.; Wong, L.S.; Mo, K.H.; Jumaat, M.Z.; Ramesh, S. A review on microstructural study and compressive strength of geopolymer mortar, paste and concrete. *Constr. Build. Mater.* **2018**, *186*, 550–576. [CrossRef]
74. Ahmad, S.; Bahraq, A.A.; Shaqraa, A.A.; Khalid, H.R.; Al-Gadhib, A.H.; Maslehuddin, M. Effects of key factors on the compressive strength of metakaolin and limestone powder-based alkali-activated concrete mixtures: An experimental and statistical study. *Case Stud. Constr. Mater.* **2022**, *16*, e00915. [CrossRef]
75. Atiş, C.D.; Görür, E.B.; Karahan, O.; Bilim, C.; Ilkentapar, S.; Luga, E. Very high strength (120 MPa) class F fly ash geopolymer mortar activated at different NaOH amount, heat curing temperature and heat curing duration. *Constr. Build. Mater.* **2015**, *96*, 673–678. [CrossRef]
76. Xiao, R.; Ma, Y.; Jiang, X.; Zhang, M.; Zhang, Y.; Wang, Y.; Huang, B.; He, Q. Strength, microstructure, efflorescence behavior and environmental impacts of waste glass geopolymers cured at ambient temperature. *J. Clean. Prod.* **2020**, *252*, 119610. [CrossRef]
77. Pommer, V.; Vejmelková, E.; Černý, R.; Keppert, M. Alkali-activated waste ceramics: Importance of precursor particle size distribution. *Ceram. Int.* **2021**, *47*, 31574–31582. [CrossRef]
78. Elie, K.; Valeria, A.; Daniele, N.; Davide, S.; Isabella, L.; Alberto, M.; Cristina, L. Dependence of the geopolymerization process and end-products to the nature of solid precursors: Challenge of the sustainability. *J. Clean. Prod.* **2021**, *278*, 123587. [CrossRef]
79. Ulugöl, H.; Kul, A.; Yıldırım, G.; Şahmaran, M.; Aldemir, A.; Figueira, D.; Ashour, A. Mechanical and microstructural characterization of geopolymers from assorted construction and demolition waste-based masonry and glass. *J. Clean. Prod.* **2021**, *280*, 124358. [CrossRef]
80. Gunasekara, C.; Law, D.W.; Setunge, S.; Sanjayan, J.G. Zeta potential, gel formation and compressive strength of low calcium fly ash geopolymers. *Constr. Build. Mater.* **2015**, *95*, 592–599. [CrossRef]
81. Tho-In, T.; Sata, V.; Boonserm, K.; Chindaprasirt, P. Compressive strength and microstructure analysis of geopolymer paste using waste glass powder and fly ash. *J. Clean. Prod.* **2016**, *172*, 2892–2898. [CrossRef]
82. Safari, Z.; Kurda, R.; Al-Hadad, B.; Mahmood, F.; Tapan, M. Mechanical characteristics of pumice-based geopolymer paste. *Resour. Conserv. Recycl.* **2020**, *162*, 105055. [CrossRef]
83. Elkafrawy, M.; Nabil, A.; Meleka, N. Development Factors in Eco-Friendly Geopolymer Concrete A State of the Art Review. *Eng. Res. J.* **2023**, *46*, 99–118. [CrossRef]
84. Gebregziabiher, B.S.; Thomas, R.J.; Peethamparan, S. Temperature and activator effect on early-age reaction kinetics of alkali-activated slag binders. *Constr. Build. Mater.* **2016**, *113*, 783–793. [CrossRef]
85. Samuvel Raj, R.; Prince Arulraj, G.; Anand, N.; Kanagaraj, B.; Lubloy, E.; Naser, M.Z. Nanomaterials in geopolymer composites: A review. *Dev. Built Environ.* **2023**, *13*, 100114. [CrossRef]
86. Sajan, P.; Jiang, T.; Lau, C.K.; Tan, G.; Ng, K. Combined effect of curing temperature, curing period and alkaline concentration on the mechanical properties of fly ash-based geopolymer. *Clean. Mater.* **2021**, *1*, 100002. [CrossRef]
87. Singh, B.; Ishwarya, G.; Gupta, M.; Bhattacharyya, S.K. Geopolymer concrete: A review of some recent developments. *Constr. Build. Mater.* **2015**, *85*, 78–90. [CrossRef]
88. Samad, S.; Shah, A.; Limbachiya, M.C. Strength development characteristics of concrete produced with blended cement using ground granulated blast furnace slag (GGBS) under various curing conditions. *Sadhana-Acad. Proc. Eng. Sci.* **2017**, *42*, 1203–1213. [CrossRef]
89. Rangan, B.V. Fly Ash-Based Geopolymer Concrete Fly Ash-Based Geopolymer Concrete. *Geopolymer Cem. Concr.* **2014**, *7982*, 68–106. [CrossRef]

90. Shilar, F.A.; Ganachari, S.V.; Patil, V.B.; Khan, T.M.Y.; Dawood Abdul Khadar, S. Molarity activity effect on mechanical and microstructure properties of geopolymer concrete: A review. *Case Stud. Constr. Mater.* **2022**, *16*, e01014. [CrossRef]
91. Adam, A.A.; Deviana, L.; Siregar, A.P.N. Mustofa Water absorption of ambient-cured geopolymer concrete. *IOP Conf. Ser. Earth Environ. Sci.* **2023**, *1157*, 12025. [CrossRef]
92. Gunasekara, C.M. Influence of Properties of Fly Ash From Different Sources on the Mix Design and Performance of Geopolymer Concrete. Ph.D. Thesis, RMIT University, Melbourne, VIC, Australia, 2016; 245p.

Disclaimer/Publisher's Note: The statements, opinions and data contained in all publications are solely those of the individual author(s) and contributor(s) and not of MDPI and/or the editor(s). MDPI and/or the editor(s) disclaim responsibility for any injury to people or property resulting from any ideas, methods, instructions or products referred to in the content.